Supplementary Methods

Isolation of ES cells with a floxed allele of the *Arg1* gene. We cloned and characterized the murine *Arg1* gene from YAC clones isolated from the Whitehead/MIT 820 YAC library [1] that contained the entire gene. *LoxP* sites were inserted into the locus such that normal *Arg1* gene expression would not be disturbed except in CRE-expressing cells. The crystal structure of rat *Arg1* [2,3] was used to guide the design of a null allele. Arg1 is a trimeric manganese-containing enzyme where each monomer has independent enzymatic activity. The C-terminal oligomerization domain of each monomer is required to hold the trimeric structure together [4]. Close to the oligomerization domain is a region encoding two highly conserved aspartic acid residues that are essential for coordination of the two Mn^{2+} ions per monomer. Biochemical studies have shown that D232 and D234 are absolutely required for enzymatic activity [3]. Therefore, we chose to target the intron adjacent to this coding region of the gene for insertion of the first *loxP* site. An additional consideration was the oligomerization domain of the protein.

A human Arg1 mutation has been described that disrupts the oligomerization rendering the protein monomeric [4], retaining ~10% of total enzyme activity. These data suggested that CRE -mediated deletion of the region encoding D232 and D234 and the oligomerization domain would result in a null allele. To insert the first *loxP* site in intron 6, primers were designed to amplify the *loxP-kanR-loxP* cassette from pUH6 [5]. This cassette was transformed into yeast containing *Arg1*-containing YACs and G418-resistant clones were obtained. Correct clones were then transformed with pSH6 carrying the *cre* gene under the control of the GAL1-10 promoter and selected on plates lacking histidine. CRE expression was induced in these strains by culture in galactose. The expression of CRE deleted the *loxP-kan-loxP* cassette and left only a single *loxP* site in the intron. This was confirmed by sequencing PCR products that flanked the *loxP* site. The strains were then cured of pSH6 by growing the yeast in the presence of histidine.

To obtain the final modified allele, YTT cassette C [6] was amplified with overlapping ends homologous to sequences in the 3'UTR downstream of the predicted polyadenylation site along with *loxP* sites at each end. This PCR product was transformed into the strains described above and selected using complementation of histidine auxotrophy of the YAC-bearing yeast strain. A large fragment of DNA was isolated from these strains using *Kpn*I and zeocin selection as described above. The cassette was removed using *Asc*I digestion and replaced with pGT-N38-

*Asc*I, a modified version of pGT-N38 (New England Biolabs) where the *Hind*III site was replaced with an *Asc*I site. Bruce4 C57BL/6 ES cells [7] were transfected with linearized versions of the targeting vector and selected with 150 µg/ml G418. Of 192 clones picked, 5 had the correct integration event as confirmed by Southern analysis of *Kpn*I digested DNA and probing with a cDNA probe encompassing the coding region from exons 3-8 (data not shown). These clones were expanded and transfected with plasmids expressing cre under the control of the CMV promoter.

A red-shifted GFP plasmid was included in the transfections to allow sorting of transfected cells. CRE transfected ES cells were sorted and plated in medium lacking G418. Clones were picked and tested for G418 sensitivity. G418 sensitive clones were then tested by PCR for the correct recombination events using primers specific for each predicted recombination event. The desired version of the allele contains the *loxP* sites in intron 7 and in the 3'UTR. PCR confirmed this result for ~10% of CRE -transfected clones. Several clones were found to be G418-sensitive and generated PCR products consistent with the presence of an $Arg1^{flox}$ allele. Chimeric male mice were crossed to female C57BL/6 mice to obtain germline transmission. These mice were then crossed to mice carrying the *LysMcre* [8] or *Tie2cre* [9] alleles that we backcrossed to the Balb/c or C57BL/6 backgrounds. $Arg1^{flox}$ mice were also backcrossed to the Balb/c background. The majority of mice used were $Arg1^{flox/flox}$*; Tie2cre* mice or $Arg1^{flox/flox}$*; LysMcre* mice backcrossed n = 6 (minimum backcross) to C57BL/6 or Balb/c. Controls were *Tie2cre*, *LysMcre* or $Arg1^{flox/flox}$ mice generated from F2 intercross breeding.

Figure S1

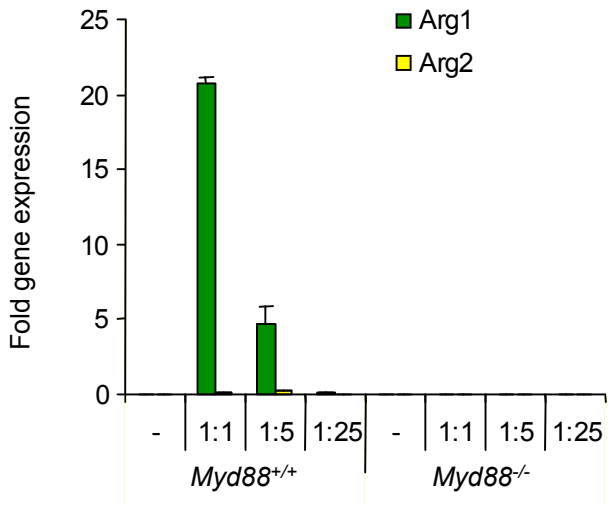

Supplemental Fig. 1. Arg1 and Arg2 mRNA expression in BCG-infected macrophages. BMDMs from *Myd88*$^{+/+}$ or *Myd88*$^{-/-}$ mice were infected in triplicate cultures with decreasing amounts of BCG in the dilutions shown on the abcissa. Arg1 and Arg2 mRNAs were quantified by qRT-PCR. Results were expressed as fold induction relative to the uninfected macrophages processed in parallel.

Figure S2

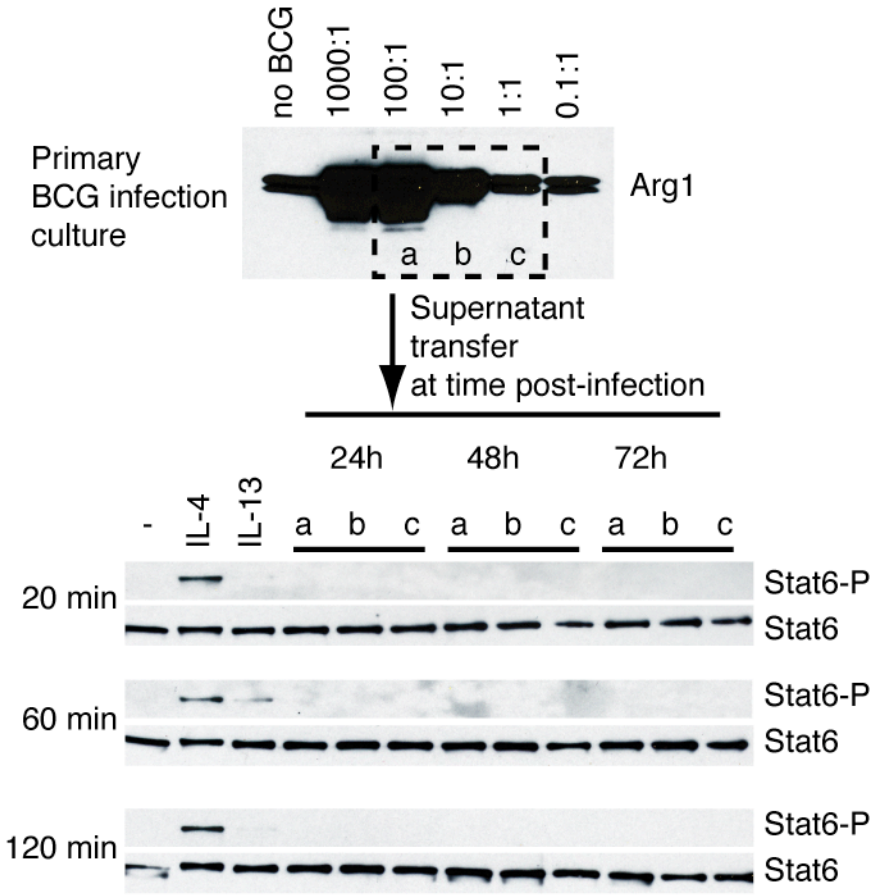

Supplemental Fig. 2. Mycobacteria-infected cultures do not produce detectable factors that can activate Stat6. To test if BCG-infected cultures produced IL-4, IL-13 or any other soluble factors that could activate STAT6, we infected C57BL/6 BMDMs with different doses of BCG as shown in the top of the figure. Arg1 expression was tested by immunoblotting (top blot) and by RT-PCR (data not shown). Cultures from infected BMDMs marked a, b and c were collected at 24, 48 and 72h post-infection, centrifuged and frozen at $^{-}$80 °C. Another set of BMDM cultures was established in 12 well plates (0.5×10^6 cell per well) and stimulated with 100 µl of culture supernatants from the BCG-infected cells (final concentration 10%) or IL-4 or IL-13 as positive controls, for times 20, 60 and 12 mins. Cells were lysed in the presence of protease and phosphatase inhibitors and analyzed by immunoblot for tyrosine phosphorylated Stat6, or upon re-probing, Stat6.

Figure S3

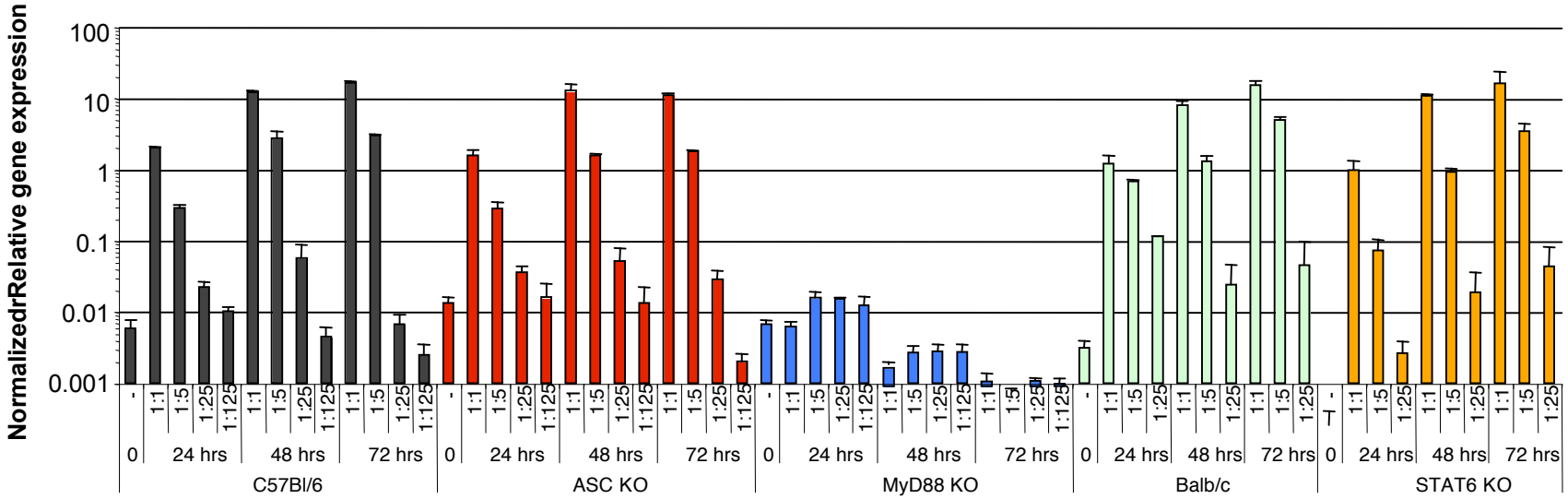

Supplemental Fig. 3. Arg1 expression in BCG-infected macrophages. Quantitative RT-PCR of Arg1 mRNA expression in C57BL/6, *Pycard*$^{-/-}$, *Myd88*$^{-/-}$, *Stat6*$^{-/-}$ or Balb/c BMDMs were infected with BCG in decreasing amounts (1:1 through 1:125 where 1:1 indicates an MOI of ~100: 1). RNA was isolated from triplicate cultures at 24, 48 and 72 hr post-infection and Arg1 mRNA was normalized to *Gapdh* mRNA. Data were expressed on a log scale (compared to **Fig. 1b** where data are expressed on a linear scale) and are representative of two independent experiments.

Figure S4

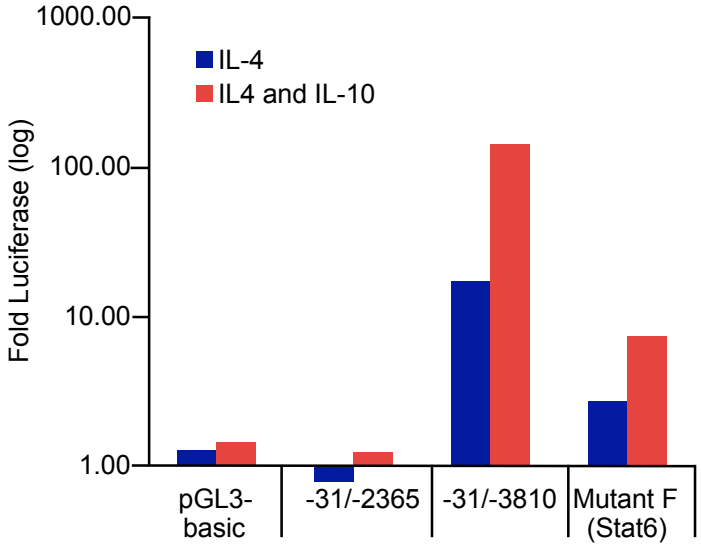

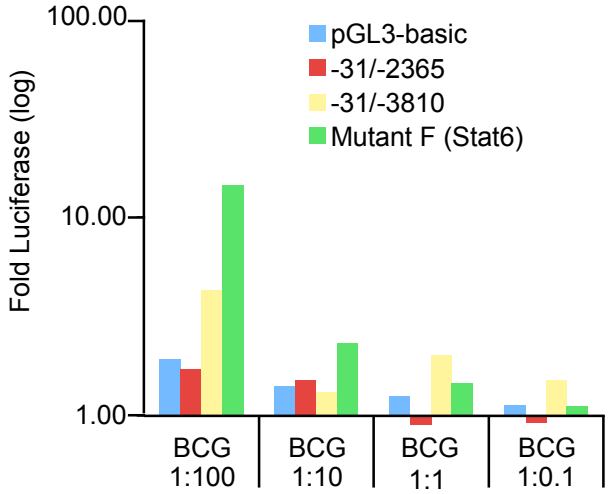

Supplemental Fig. 4. BCG-mediated activation of Arg1 expression does not require the Stat6 binding site in the Arg1 enhancer. RAW cells were transiently transfected with 10 µg of the reporter constructs shown (pGL3, empty luciferase reporter; -31/-2365 basal *Arg1* promoter; -31/-3810 *Arg1* basal promoter/enhancer; mutant F, a variant of -31/-3810 with a 4 nucleotide mutation in the STAT6 binding site of the enhancer) [10,11]. Twenty four hours following the transfection, RAW cells were infected with different amounts of BCG as shown and 24h later, luciferase reporter activity measured. (Left panel) Internal controls with IL-4 or IL-4+IL-10 stimulation to demonstrate that IL-4-mediated expression via STAT6 is almost completely ablated in Mutant F consistent with previous data [10,11]. (Right panel) Induction of luciferase activity by BCG or LPS is unaffected in cells transfected with Mutant F. Data are one of two independent experiments were each sample was measured in duplicate and the data averaged. Lower panel: schematic representation of the pathways for *Arg1* expression in macrophages showing the common use of C/EBPβ.

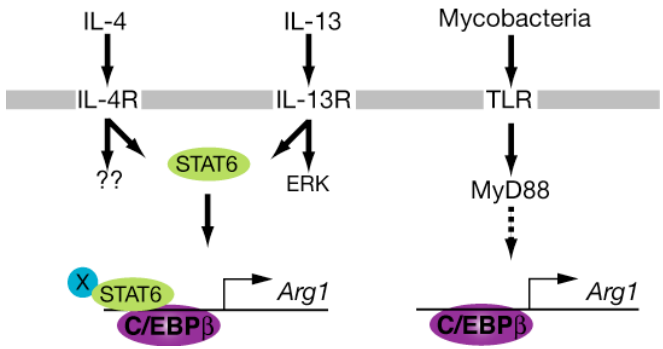

Figure S5

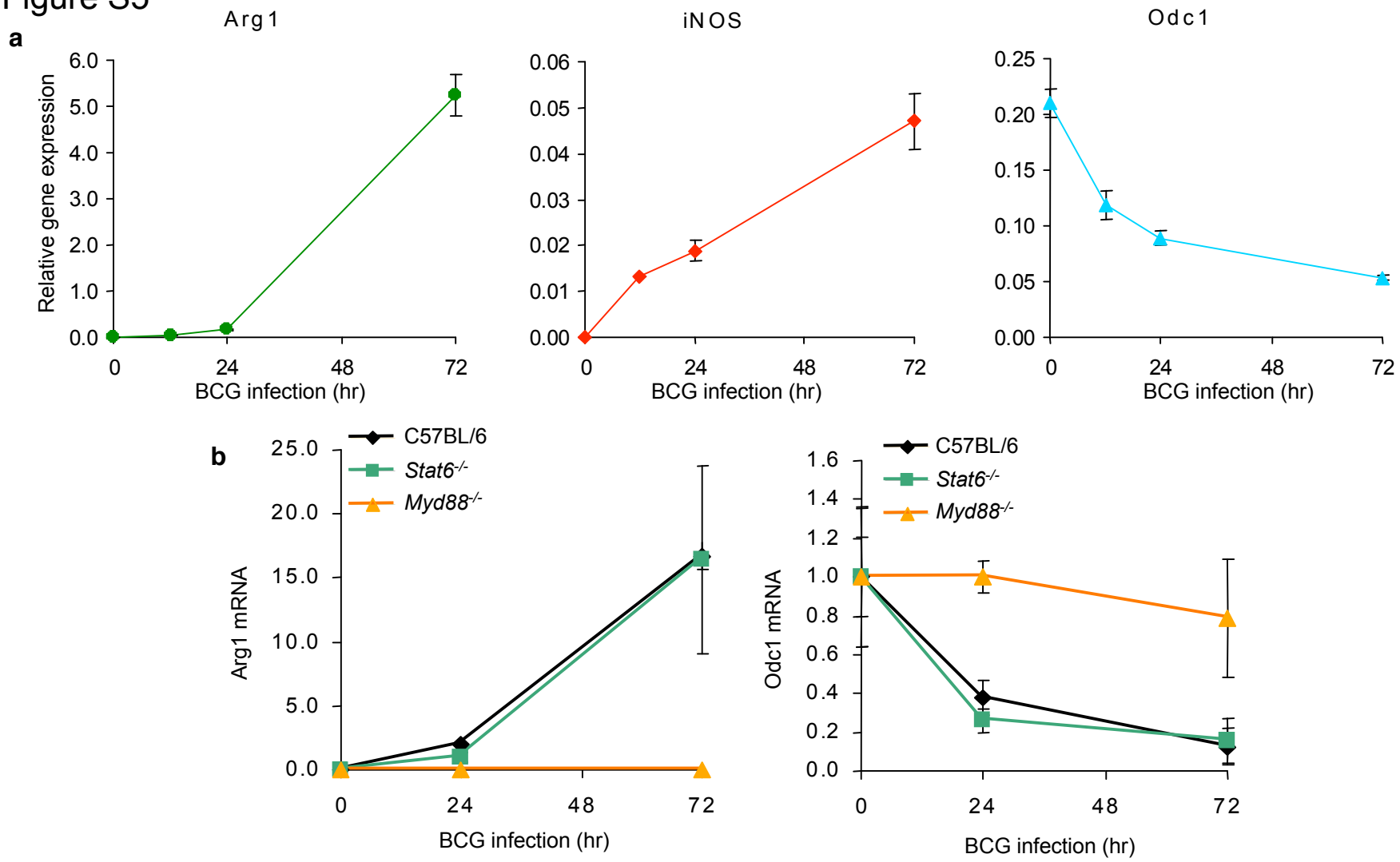

Supplemental Fig. 5. Arg1, Arg2 and Odc expression in BCG-infected BMDMs. (**a**) Relative quantification of Arg1, iNOS and Odc mRNA amounts in BCG infected BMDMs. (**b**) BMDMs from C57BL/6, *Stat6*$^{-/-}$ or *Myd88*$^{-/-}$ mice were infected in triplicate cultures with decreasing BCG. Arg1 and Odc mRNAs were quantified by qRT-PCR. Results were expressed as fold induction relative to the uninfected macrophages processed in parallel. Data are representative of four independent experiments.

Figure S6

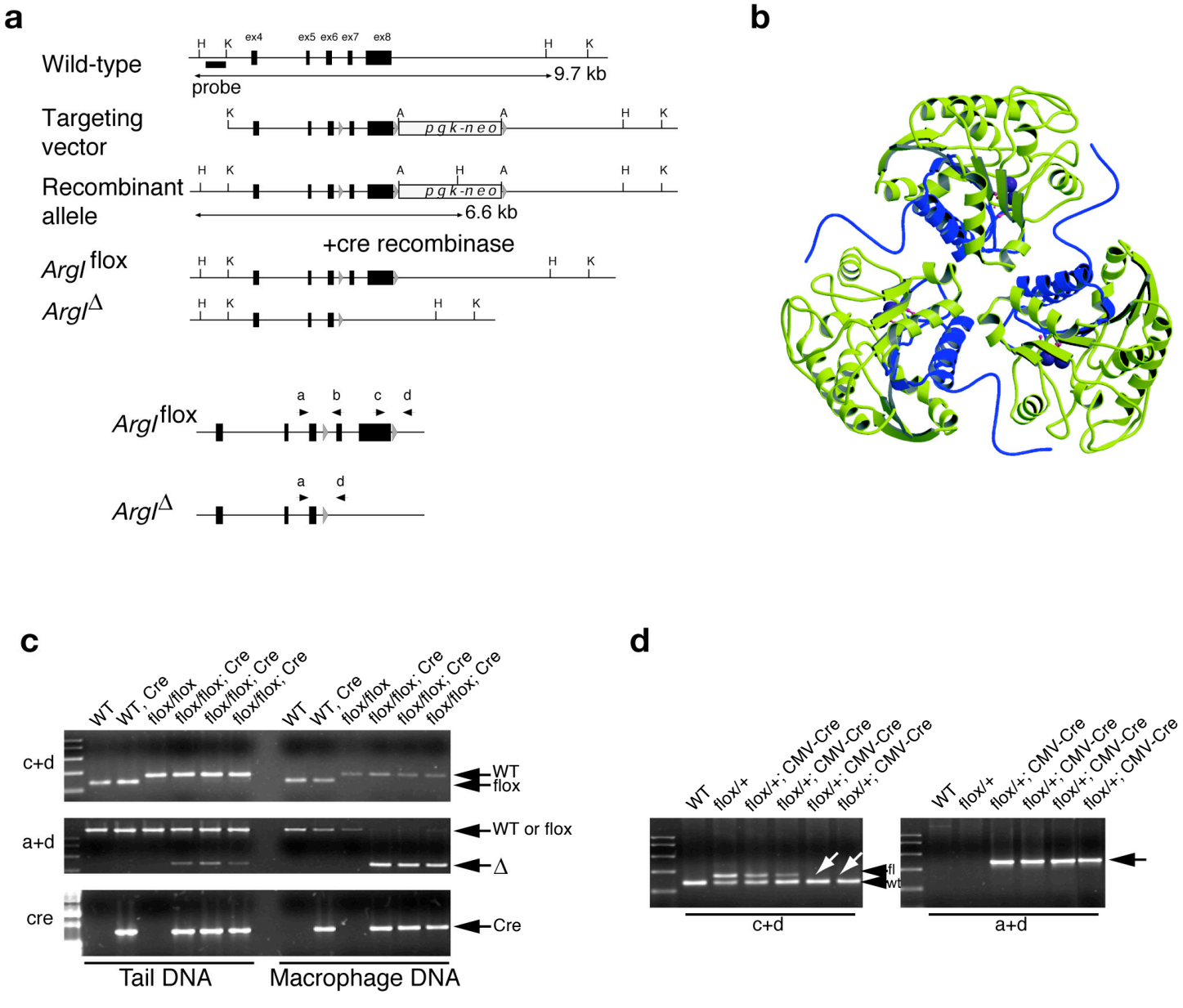
a
Wild-type
probe
9.7 kb
Targeting vector
pgk-neo
Recombinant allele
6.6 kb
+cre recombinase
Argl flox
Argl Δ
b
c
WT
WT, Cre
flox/flox
flox/flox; Cre
c+d
a+d
cre
WT or flox
Δ
Cre
Tail DNA
Macrophage DNA
d
flox/+
flox/+; CMV-Cre
fl
wt
c+d
a+d

Supplemental Fig. 6. Construction of a conditional allele of *Arg1*. (**a**) Diagram of the *Arg1* locus and its modification. Shown is the targeting vector, the resulting recombinant allele, the allele following Cre-mediated modification to leave two *loxP* sites and the locus after Cre-recombination to delete exons 7 and 8. Shown at the bottom is the location of primers designed to distinguish between the different alleles. (**b**) Ribbon diagram of the rat Arg1 trimer showing the buried Mn^{2+} ions (purple balls) and the region designed to be deleted in the mature protein (blue) which includes the coordination sites for the metal ions and the C-terminal oligomerization domain. (**c**) PCR-based genotyping of mice and macrophages derived from Arg1flox mice crossed to the *lysMcre* deleter strain. Primers c + d detect the wild-type or floxed allele while primers a + d detect the wild-type or Δ allele. Note that the Δ allele can be detected in tail DNA because of the presence of macrophages and neutrophils in the tail (middle panel). The Δ allele is enriched in macrophage genomic DNA because of the enriched activity of the Cre recombinase. (**d**) Derivation of mice with a complete null allele at *Arg1*. $Arg1^{flox/+}$ mice were crossed with *CMV-cre* mice. Cre activity in these animals occurs in all tissues including the germline. F1 mice were screened for mice bearing high deletion of the floxed allele (and hence retaining one Δ and one wild-type allele). Male mice with high deletion of the floxed allele were then crossed to female C57BL/6 mice to derive pure $Arg1^{\Delta/+}$ mice. The CMV-cre alleles are sex-linked and were removed by intercrossing. The resulting mice (right panel) were pure $Arg1^{\Delta/+}$ and were intercrossed to generate embryos that were $Arg1^{\Delta/\Delta}$.

Figure S7

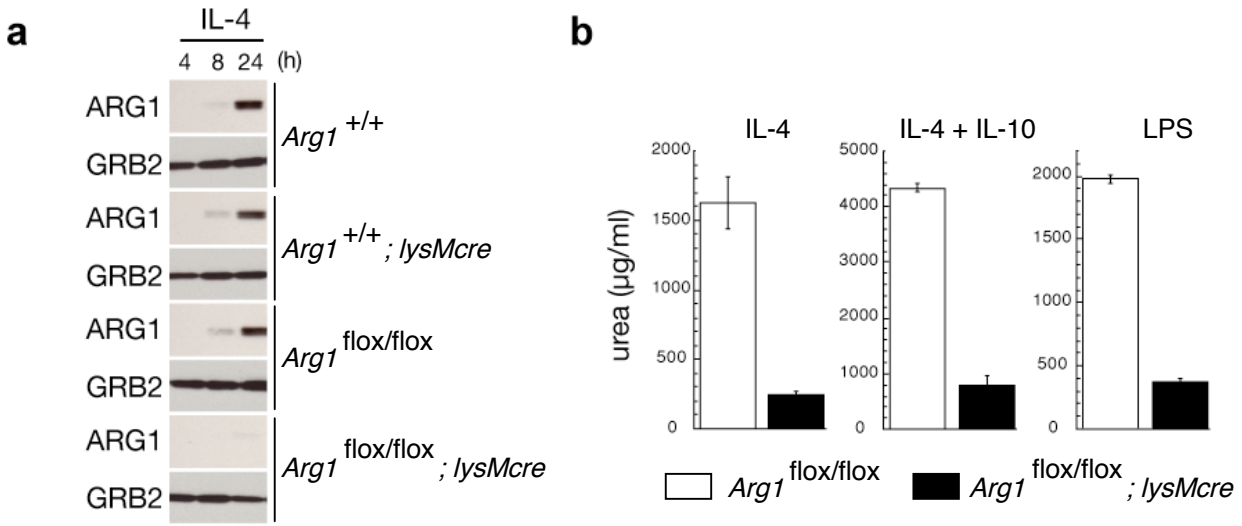

Supplemental Fig. 7. Depletion of Arg1 in macrophages using the *lysMcre* deleter strain. (**a**) Immunoblots from BMDMs stimulated with IL-4 for 4, 8 and 24 h isolated from the strains shown. GRB2 was used as a loading control. (**b**) Arginase enzyme activity following stimulation with IL-4, IL-4+IL-10 or LPS in BMDMs isolated from control or ARG1-deficient mice where the *lysMcre* deleter strain was employed. Data represent means ± s.d. from triplicate wells from n = 3 mice.

Figure S8

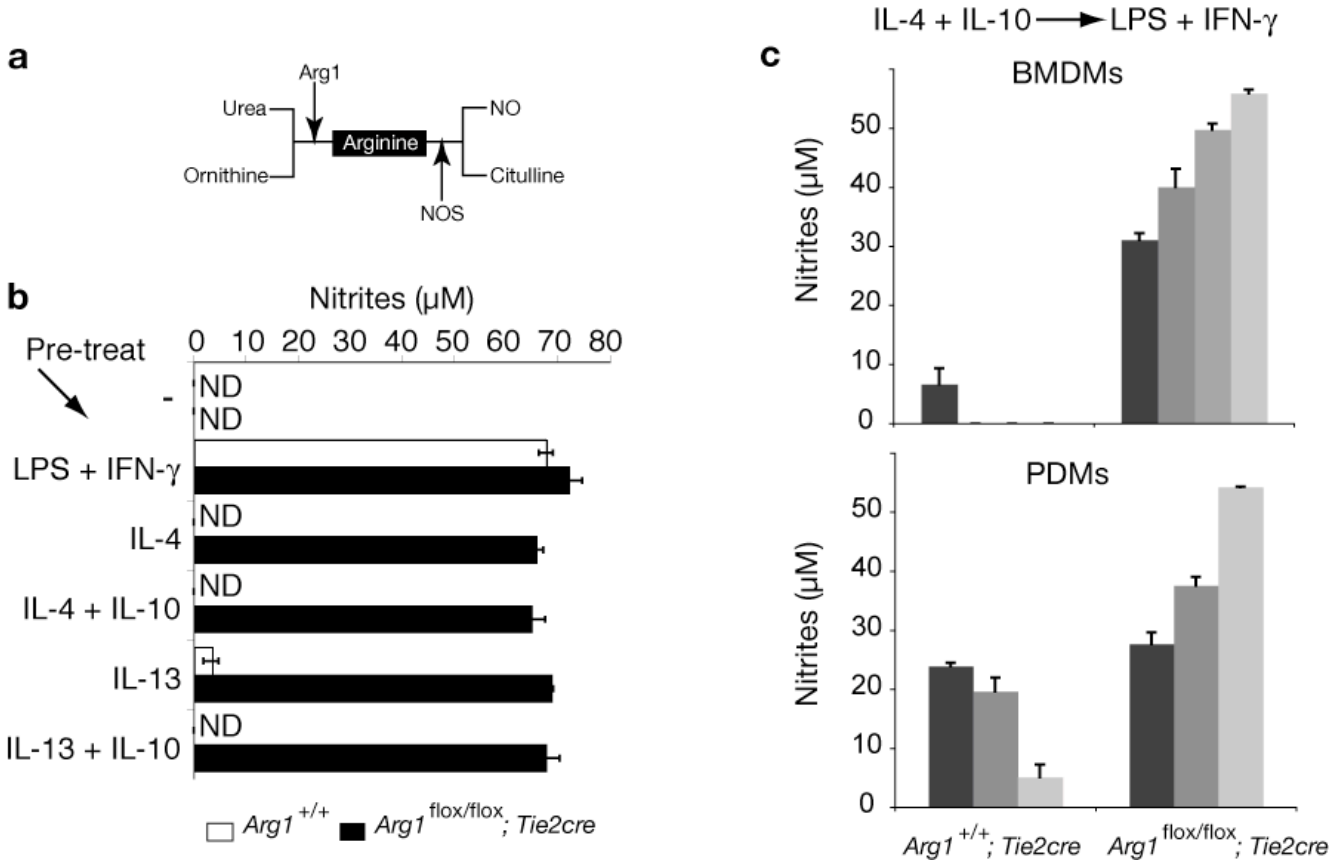

Supplemental Figure 8. Arg1 controls NO production. (**a**) Simplified pathway diagram illustrating the use of arginine by Arg1 and iNOS, and the products from each reaction. (**b**) Arg1 is the only factor required to block NO production from IL-4 or IL-13 stimulated macrophages. BMDMs from *Arg1*$^{flox/flox}$*; Tie2cre* mice (black bars) or control mice (open bars) were stimulated for 16 h with the stimuli shown on the ordinate at concentrations as described [12]. After 16 h, all cultures except the untreated controls (–) were restimulated with LPS + IFN-γ for a further 12 h and nitrites in the culture supernatants measured by the Griess assay (ND, not detected, error bars s.d. from $n = 4$ samples). (**c**) As in (**b**) except that increasing amounts of cells (depicted in order of dark to light bars) were plated in 24-well plates (top panel: 0.2×10^6, 0.4×10^6, 0.6×10^6 and 0.8×10^6; bottom panel: 0.2×10^6, 0.4×10^6, and 0.8×10^6) and stimulated with IL-4+IL-10 and re-stimulated with LPS + IFN-γ. Data are mean values ± s.d. from quadruplicate wells that are representative of three independent experiments. (**e,f**) Arg1-deficient macrophages produce increased NO after LPS stimulation. BMDMs (panel **e**) or fetal liver-derived macrophages (panel **f**) from the genotypes shown were stimulated with LPS for 24 hr and re-stimulated with LPS + IFN-γ for a further 16 hr and nitrite measured in the cell supernatants. Means ± s.d. from quadruplicate samples are shown.

Figure S9

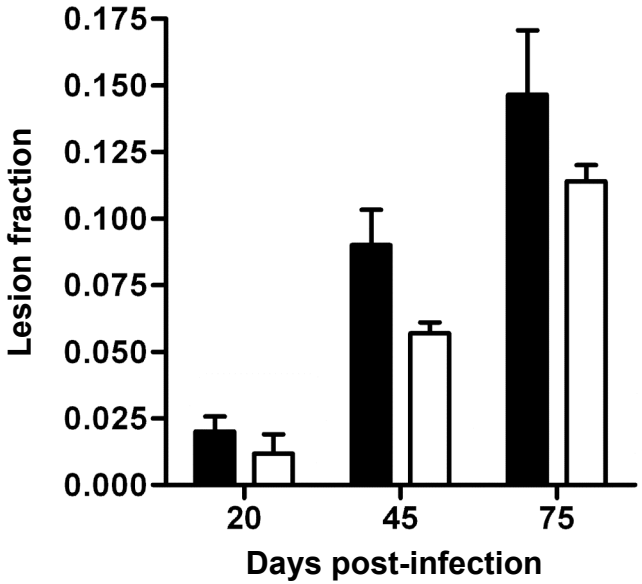

Supplemental Figure 9. Morphometric measurement of lesion size in TB-infected lungs. Total area of lesions in the lungs was measured by morphometry. Data are expressed as the volume fraction of the lung area occupied by TB-induced histopathological lesions over time (days) using sections cut from the experiment described in Fig. 4.

Figure S10

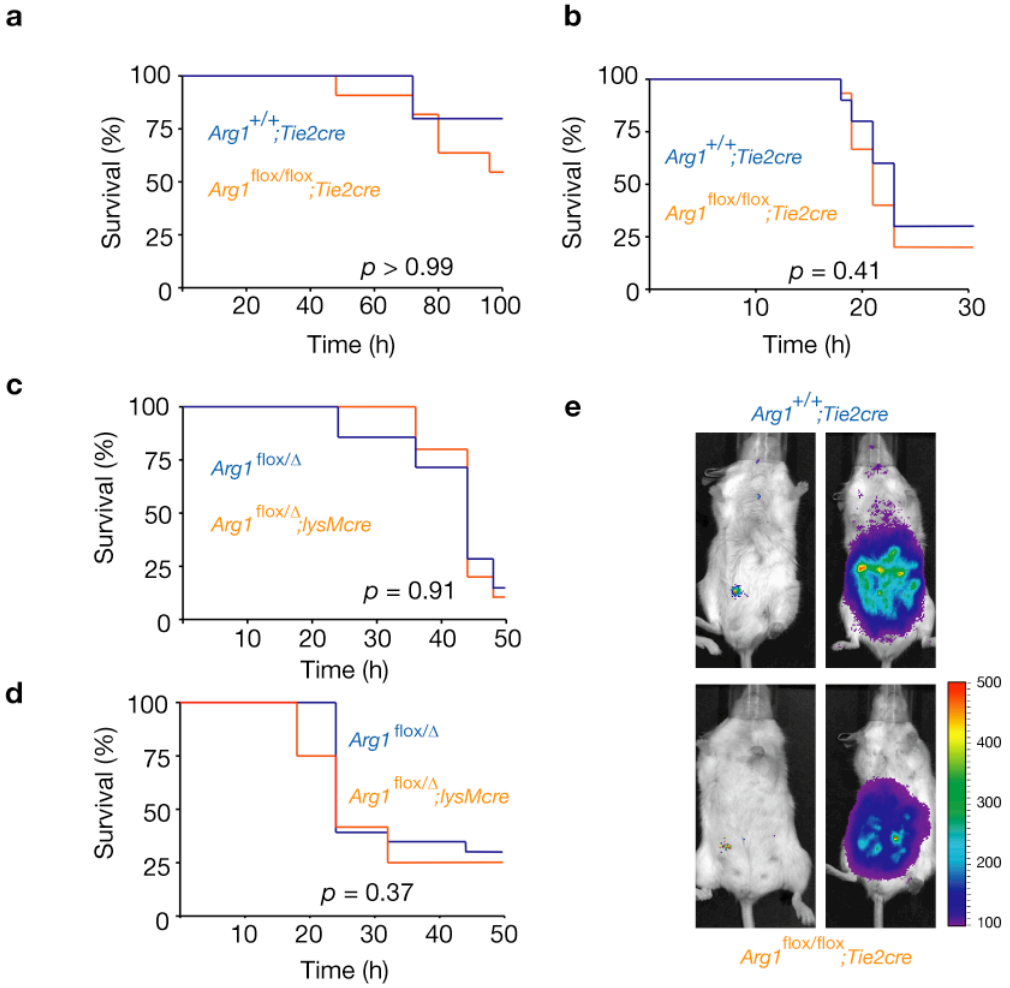

Supplemental Figure 10. LPS and *S. pneumoniae* challenges in macrophage Arg1-deficient mice on the lysMcre background deleter strain. (a-d) Kaplan-Meier plots depicting survival responses following challenge with LPS (35 mg/kg) in macrophage Arg1-deficient mice (*Tie2cre* deleter strain, panel **b**; *LysMcre* deleter strain, **a** (n = 10-12, per experiment). Results are representative of 10 experiments titrating LPS doses above or below 35 mg/kg. (**b,d**) Kaplan-Meier plots depicting survival responses following challenge with *S. pneumoniae* D39X via the intranasal route (n = 6-8 mice per group). Results are representative of 4 independent experiments that titrated doses of bacteria administered into the airways. No statistically significant differences were noted in any experiments assuming a $p < 0.05$ as significant. (**e**) Representative images of intraperitoneal luciferase-transduced *S. pneumoniae* D39X infections showing control or *Arg1*$^{flox/flox}$*; Tie2cre* mice infected at 1 h (left panels) or 2 days after infection.

References

1. Kusumi, K., Smith, J.S., Segre, J.A., Koos, D.S. & Lander, E.S. Construction of a large-insert yeast artificial chromosome library of the mouse genome. *Mamm Genome* **4**, 391-392 (1993).
2. Kanyo, Z.F., Chen, C.Y., Daghigh, F., Ash, D.E. & Christianson, D.W. Crystallization and oligomeric structure of rat liver arginase. *J Mol Biol* **224**, 1175-1177 (1992).
3. Kanyo, Z.F., Scolnick, L.R., Ash, D.E. & Christianson, D.W. Structure of a unique binuclear manganese cluster in arginase. *Nature* **383**, 554-557 (1996).
4. Lavulo, L.T.*, et al.* Subunit-subunit interactions in trimeric arginase. Generation of active monomers by mutation of a single amino acid. *J Biol Chem* **276**, 14242-14248 (2001).
5. Guldener, U., Heck, S., Fielder, T., Beinhauer, J. & Hegemann, J.H. A new efficient gene disruption cassette for repeated use in budding yeast. *Nucleic Acids Res* **24**, 2519-2524 (1996).
6. Wilson, C.J.*, et al.* Yeast artificial chromosome targeting technology: an approach for the deletion of genes in the C57BL/6 mouse. *Anal Biochem* **296**, 270-278 (2001).
7. Kontgen, F., Suss, G., Stewart, C., Steinmetz, M. & Bluethmann, H. Targeted disruption of the MHC class II Aa gene in C57BL/6 mice. *Int Immunol* **5**, 957-964 (1993).
8. Clausen, B.E., Burkhardt, C., Reith, W., Renkawitz, R. & Forster, I. Conditional gene targeting in macrophages and granulocytes using LysMcre mice. *Transgenic Res* **8**, 265-277 (1999).
9. Kisanuki, Y.Y.*, et al.* Tie2-Cre transgenic mice: a new model for endothelial cell-lineage analysis in vivo. *Dev Biol* **230**, 230-242 (2001).
10. Pauleau, A.L.*, et al.* Enhancer-mediated control of macrophage-specific arginase I expression. *J Immunol* **172**, 7565-7573 (2004).
11. Vats, D.*, et al.* Oxidative metabolism and PGC-1beta attenuate macrophage-mediated inflammation. *Cell Metab* **4**, 13-24 (2006).
12. Rutschman, R.*, et al.* Cutting edge: Stat6-dependent substrate depletion regulates nitric oxide production. *J Immunol* **166**, 2173-2177 (2001).